NEOPLASIA
www.neoplasia.com

Volume 20 Number 2 February 2018 pp. 197–206 197

Anti-cancer Effects of HNHA and Lenvatinib by the Suppression of EMT-Mediated Drug Resistance in Cancer Stem Cells[1,2]

Yong Sang Lee[*,†,3], Seok-Mo Kim[*,†,3], Bup-Woo Kim[*,†], Ho Jin Chang[*,†], Soo Young Kim[*,†], Cheong Soo Park[*,†], Ki Cheong Park[*,‡,3] and Hang-Seok Chang[*,†,3]

*Thyroid Cancer Center, Gangnam Severance Hospital, Department of Surgery, Yonsei University College of Medicine, Seoul 120-752, Korea; [†]Gangnam Severance Hospital, Department of Surgery Yonsei University College of Medicine 211 Eonjuro, Gangnam-gu, Seoul 135-720, Korea; [‡]Department of Surgery, Yonsei University College of Medicine, 50-1, Yonsei-ro, Seodaemun-gu, Seoul, 120-752 Korea

Abstract

Anaplastic thyroid cancer (ATC) constitutes less than 2% of total thyroid cancers but accounts for 20–40% of thyroid cancer-related deaths. Cancer stem cell drug resistance represents a primary factor hindering treatment. This study aimed to develop targeted agents against thyroid malignancy, focusing on individual and synergistic effects of HNHA (histone deacetylase), lenvatinib (FGFR), and sorafenib (tyrosine kinase) inhibitors. Patients with biochemically and histologically proven papillary thyroid cancer (PTC) and ATC were included. Cell samples were obtained from patients at the Thyroid Cancer Center, Gangnam Severance Hospital, Yonsei University College of Medicine, Seoul, Korea. PTC and ATC cells were treated with lenvatinib or sorafenib, alone or in combination with HNHA. Tumor-bearing mice (10/group) were administered 10 mg/kg lenvatinib (p.o.) or 40 mg/kg sorafenib (p.o.), alone or in combination with 25 mg/kg HNHA (i.p.) once every three days. Gene expression in patient-derived PTC and ATC cells was compared using a microarray approach. Cellular apoptosis and proliferation were examined by immunohistochemistry and MTT assays. Tumor volume and cell properties were examined in the mouse xenograft model. HNHA-lenvatinib combined treatment induced markers of cell cycle arrest and apoptosis and suppressed anti-apoptosis markers, epithelial-mesenchymal transition (EMT), and the FGFR signaling pathway. Combined treatment induced significant tumor shrinkage in the xenograft model. HNHA-lenvatinib combination treatment thus blocked the FGFR signaling pathway, which is important for EMT. Treatment with HNHA-lenvatinib combination was more effective than either agent alone or sorafenib-HNHA combination. These findings have implications for ATC treatment by preventing drug resistance in cancer stem cells.

Neoplasia (2018) 20, 197–206

Abbreviations: ATC, anaplastic thyroid cancer; EMT, epithelial-mesenchymal transition; PTC, papillary thyroid cancer; TKI, tyrosine kinase inhibitors.

Address all correspondence to: Hang-Seok Chang, M.D., Ph.D., Gangnam Severance Hospital, Department of Surgery, Yonsei University College of Medicine, 211 Eonjuro, Gangnam-gu, Seoul 135-720, Korea. E-mail: SURGHSC@yuhs.ac or Ki Cheong Park., Ph. D., Department of Surgery, Yonsei University College of Medicine, 50-1, Yonsei-ro, Seodaemun-gu, Seoul 120-752, Republic of Korea. Email: ggiru95@yuhs.ac

[1] Funding: This research was supported by he "SEBANG" Faculty Research Assistance Program of Yonsei University College of Medicine 6-2013-0160 and the Basic Science Research Program through the National Research Foundation of Korea (NRF) funded by the Ministry of Education (NRF-2017R1D1A1B03029716).

[2] Conflicts of interest: The authors declare that they have no competing interests.

[3] These authors contributed equally to this work.

Received 16 September 2017; Revised 12 December 2017; Accepted 14 December 2017

1476-5586
https://doi.org/10.1016/j.neo.2017.12.003

Introduction

Thyroid cancer represents more than 90% of all endocrine cancer cases, and its incidence has increased over the past three decades [1,2]. Thyroid cancer encompasses a broad scope of tumors derived from follicular cells that range from well-differentiated papillary (PTC) and follicular cancer (FTC), which generally have a favorable prognosis, through anaplastic thyroid cancer, a clinically aggressive form with poor prognosis, including poorly differentiated (PDTC) and undifferentiated thyroid cancer [3–5]. In particular, the advanced cancer subtype (ATC) has a poor prognosis owing to its resistance to treatment and aggressive behavior [5,6]. The total median survival is only a few months [6,7].

Poorly differentiated cancers are often resistant to anti-cancer drugs; moreover, effective clinical guidelines for ATC are currently lacking [7]. However, recent evidence has shown that induction of the epithelial-mesenchymal transition (EMT) in cancer cells not only results in metastasis, but also serves as a major contributing factor in drug resistance [8,9]. Nevertheless, the mechanisms of EMT-mediated drug resistance remain unclear. EMT is a physiological process in which epithelial cells exhibit collapse of cell–cell junctions and temporary or permanent transition to a condition that is characteristic of migratory cells [10]. Although EMT constitutes a fundamental aspect of resistance to ErbB-targeting compounds, a lack of knowledge regarding the molecular mechanisms underlying this process has prevented progress in the development of therapeutic approaches targeting this drug-resistant state [11,12]. Previous research has shown that fibroblast growth factor receptor 1 (FGFR1) expression is significantly induced during TGF-β-mediated EMT and plays a crucial role in metastatic cancer [13–15]. These previous studies suggest that the drug resistance of poorly differentiated cancer stem cells (CSCs) is related to EMT, which is mediated by the FGFR signaling pathway [16,17]. Although various molecules and mechanisms are closely associated with poor clinical outcomes for advanced thyroid cancer [18,19], we focused on EMT and drug resistance in CSCs to explain these poor clinical results [8,20]. In particular, in this study we examined the mechanisms underlying drug resistance, including FGFR signaling and EMT, in response to current treatments and methods to address the issues associated with resistance.

Materials and Methods

Patients and Tissue Specimens

Fresh tumors were obtained from patients with biochemical and histologically proven PTC and ATC who were treated at the Thyroid Cancer Center, Gangnam Severance Hospital, Yonsei University College of Medicine, Seoul, Korea. Fresh tumors were acquired during surgical resection of thyroid cancer primary and metastatic sites. Several patients with thyroid cancer were chosen depending on cancer subtype. The research protocol was approved by the Institutional Review Board of the Thyroid Cancer Center, Gangnam Severance Hospital, Yonsei University College of Medicine (IRB Protocol: 3–2016-0076).

Tumor Cell Isolation and Primary Culture

After resection, tumors were kept in normal saline with antifungal and antibiotics and moved to the laboratory. Normal tissue and fat were removed and the tissues were rinsed with 1× Hank's Balanced Salt Solution. Tumors were minced in a tube with dissociation medium containing DMEM/F12 with 20% fetal bovine serum supplemented with 1 mg/ml collagenase type IV (Sigma, St. Louis, MO; C5138). Minced and suspended tumor cells were filtered through sterile nylon cell strainers with 70-micron pores (BD Falcon, Franklin Lakes, NJ, USA), rinsed with 50 ml of 1× Hank's Balanced Salt Solution, and centrifuged at 220 *g* for 5 minutes. Cells were resuspended in RPMI-1640 (Hyclone, South Logan, UT) medium with 10% fetal bovine serum (Hyclone) and 2% penicillin/streptomycin solution (Gibco, Grand Island, NY, USA). Cell viability was determined using the trypan blue dye exclusion method.

Cell Culture

The patient-derived PTC, ATC and resistance to sorafenib ATC cells were isolated and grown in RPMI-1640 medium with 10% fetal bovine serum (cells were authenticated by short tandem repeat profiling, karyotyping, and isoenzyme analysis).

Cell Viability Assay

Cell proliferation was measured using the MTT assay. Cells were seeded in 96-well plates at 6×10^3 cells per well and incubated overnight to achieve 80% confluency. The indicated drugs were added to achieve final concentrations of 0–100 μM. Cells were incubated for the indicated times prior to the determination of cell viability using the MTT reagent according to the manufacturer's protocol (Roche, Basel, Switzerland; 11,465,007,001). Absorbance was measured at 550 nm. Viable cells were counted by trypan blue exclusion. Data were expressed as a percentage of the signal observed in vehicle-treated cells and are shown as the means ± SEM of triplicate experiments.

Microarray Experiment and Data Analysis

RNA purity and integrity were evaluated using an ND-1000 Spectrophotometer (NanoDrop, Wilmington, DE) and an Agilent 2100 Bioanalyzer (Agilent Technologies, Palo Alto, CA). RNA labeling and hybridization were performed by using the Agilent One-Color Microarray-Based Gene Expression Analysis protocol (Agilent Technology, V 6.5, 2010). Briefly, 100 ng of total RNA from each sample was linearly amplified and labeled with Cy3-dCTP. The labeled cRNAs were purified using an RNAeasy Mini Kit (Qiagen, Venlo, The Netherlands). The concentration and specific activity of the labeled cRNAs (pmol Cy3/μg cRNA) were measured using the NanoDrop ND-1000. Then, 600 ng of each labeled cRNA was fragmented by adding 5 μl 10× blocking agent and 1 μl of 25× fragmentation buffer, and then heated at 60 °C for 30 minutes. Finally, 25 μl of 2× GE hybridization buffer was added to dilute the labeled cRNA. Hybridization solution (40 μl) was dispensed into the gasket slide and assembled to the Agilent SurePrint G3 Human GE 8X60K, V3 Microarrays (Agilent®). Raw data were extracted using Agilent Feature Extraction Software (v11.0.1.1). The raw data for each gene were then summarized automatically in an Agilent feature extraction protocol to generate the raw data text file, providing expression data for each gene probed on the array. Gene-enrichment and functional annotation analysis for the significant probe list was performed using gene ontology (www.geneontology.org/) and Kyoto Encyclopedia for Genes and Genomes (KEGG) (http://kegg.jp) analyses. All data analysis and visualization of differentially expressed genes were conducted using R 3.1.2 (www.r-project.org).

Immunofluorescence Analysis and Confocal Imaging

The expression of β-catenin was analyzed by immunofluorescence staining. Cells grown on glass-bottomed dishes (MatTek, Ashland,

MA) were fixed with 4% formaldehyde solution (R&D Systems, Abingdon, UK) for 10 minutes and permeabilized with 0.5% TritonX-100 in phosphate buffered saline (PBS) for 10 minutes. Slides were air-dried, washed with PBS, and incubated with anti-β-catenin (1:25; Abcam, Cambridge, UK) in 3% bovine serum albumin in PBS. After being washed with PBS, slides were incubated with Alexa 488 (1:200; Molecular Probes, Eugene, OR) Nuclei were stained with Hoechst 33,342 (Life Technologies, Grand Island, NY) for visualization. Images were observed under a confocal microscope (LSM Meta 700; Zeiss, Oberkochen, Germany) and were analyzed using Zeiss LSM Image Browser, version 4.2.0121.

Immunoblot Analysis

Cells were washed twice with cold PBS and lysed on ice with protein extraction buffer (Pro-Prep, iNtRON Biotechnology, Seoul, Korea) following the manufacturer's protocol. Protein concentrations were determined by a BCA assay (Pierce Biotechnology, Rockford, IL). Equal amounts of protein (20 μg) were separated on 8–10% sodium dodecyl sulfate-polyacrylamide gels; the resolved proteins were electro-transferred onto polyvinylidene fluoride membranes (Millipore, Bedford, MA). The membranes were subsequently blocked with 5% nonfat milk in TBS-T for 1 hour at room temperature and incubated with appropriate concentrations of primary antibodies against Ki-67, Vimentin, E-cadherin, Apaf-1, Snail, Zeb1 (all from Abcam), Cyclin D1, CDK4, p21, p53, p-ERK 1/2, ERK 1/2, p-NFκB, Bcl-2, Caspase 3, and β-actin (all from Santa Cruz Biotechnology, Dallas, TX) overnight at 4 °C. The membranes were then rinsed 3–5 times with TBST and probed with the corresponding secondary antibodies conjugated to horse radish peroxidase (Santa Cruz) at room temperature for 1 hour. After rinsing, blots were developed with ECL reagents (Pierce) and exposed using Kodak X-OMAT AR Film (Eastman Kodak, Rochester, NY) for 3–5 minutes.

Flow Cytometry Analysis of the Cell Cycle

Cells were treated with sorafenib and lenvatinib alone or in combination in RPMI-1640 medium containing 10% fetal bovine serum for 40 hours, harvested by trypsinization, and fixed with 70% ethanol. Cells were stained for total DNA using PBS containing 40 μg/ml propidium iodide and 100 μg/ml RNase I for 30 minutes at 37 °C. The cell cycle distribution was then analyzed using the FACSCalibur Flow Cytometer (BD Biosciences, San Jose, CA). The proportions of cells in the sub-G0/G1, G0/G1, S, and G2/M phases were analyzed using FlowJo v8 for MacOSX (Tree Star, Ashland, OR). This experiment was repeated in triplicate and the results were averaged.

Human Thyroid Cancer Cell Xenografts

The patient-derived PTC and ATC cells (3.5×10^6 cells/mouse) were cultured in vitro and then injected subcutaneously into the upper left flank region of female BALB/c nude mice. After 11 days, tumor-bearing mice were assigned to groups randomly (n = 10/group) and administered 10 mg/kg lenvatinib (p.o.) and 40 mg/kg sorafenib (p.o.), either alone or in combination with 25 mg/kg HNHA (given i.p.) once every 2 days. Tumor size was measured every three day using calipers. Tumor volume was estimated using the following formula: L × S2/2 (L, longest diameter; S, shortest diameter). Animals were maintained under specific pathogen-free conditions. All experiments were approved by the Animal Experiment Committee of Yonsei University.

Immunohistochemistry

All tissues were fixed in 10% neutral-buffered formalin and embedded in paraffin wax following standard protocols. Tissue sections (5 μm) were dewaxed, and antigen retrieval was performed in citrate buffer (pH 6), using an electric pressure cooker set at 120 °C for 5 minutes. Sections were incubated for 5 minutes in 3% hydrogen peroxide to quench endogenous tissue peroxidase. All tissue sections were counterstained with hematoxylin, dehydrated, and mounted.

Statistical Analysis

Statistical analyses were performed using GraphPad Prism (GraphPad Software Inc., La Jolla, CA). Immunohistochemistry results were evaluated by ANOVA followed by Bonferroni *post-hoc* tests. Values are expressed as the means ± SD. $P < .05$ indicated statistical significance.

Results

FGFR Signaling Pathway and EMT Marker Expression are Higher in PDTC than in DTC

Given that gene expression is largely dependent on the cancer subtype, we considered that CSCs achieve a stem-like phenotype by transcriptional reprogramming. We performed a gene expression microarray analysis to compare PDTC (GSA1 and GSA2) and DTC (GSP1 and GSM1) patient-derived thyroid cancer cells (Figure 1*A*). Many genes were significantly differentially expressed between PDTC and DTC cells, suggesting that multiple biological processes were reprogrammed depending on cancer cell differentiation. Genes related to FGFR and EMT were particularly induced in PDTC (Figure 1*A*). Consequently, we focused on the mechanism by which drug resistance is acquired via the FGFR signaling pathway and EMT. Patient-derived GSA1/2, GSP1, and GSM1 cells were used to analyze the expression of genes related to human diseases (Figure 1*B*). Expression patterns in patient-derived thyroid cancer cells were not significantly different from those of other thyroid cancers, including endometrial cancer. Together, these data show that genes related to the FGFR signaling pathway and EMT are expressed more highly in PDTC than in DTC.

Synergistic Effects of HNHA and Lenvatinib on Cancer Cell Proliferation in Patient-Derived Thyroid Cancer Cells

To investigate the synergistic anticancer effects of sorafenib or lenvatinib with HNHA on patient-derived PTC and ATC, we assayed GSP1, GSA1, and GSA2 (Table 1, Information for PTC and ATC from Gangnam Severance Hospital) cell proliferation in the presence and absence of these compounds by MTT assays (Figure 2*A*, *C*, and *E*). IC_{50} was lowest for the combination of HNHA and lenvatinib among all treatment groups for GSP1, GSA1, and GSA2 (Table 2). Further characterization of the synergistic effect of HNHA and lenvatinib on GSP1, GSA1, and GSA2 cell viability showed that the combination reduced the viability of PTC and ATC cells to a greater extent than the reduction observed for either agent alone or the combination of HNHA and sorafenib. The combination of HNHA and lenvatinib suppressed cell proliferation more effectively than either agent used singly or the combination of HNHA and sorafenib (Figure 2*A*, *C*, and *E*); moreover, this effect was concentration-dependent (Figure 2*B*, *D*, and *F*). Collectively, these results imply that the synergistic effect of HNHA and lenvatinib is more potent that the effects of either agent alone or the combination of HNHA and sorafenib in patient-derived PTC and ATC.

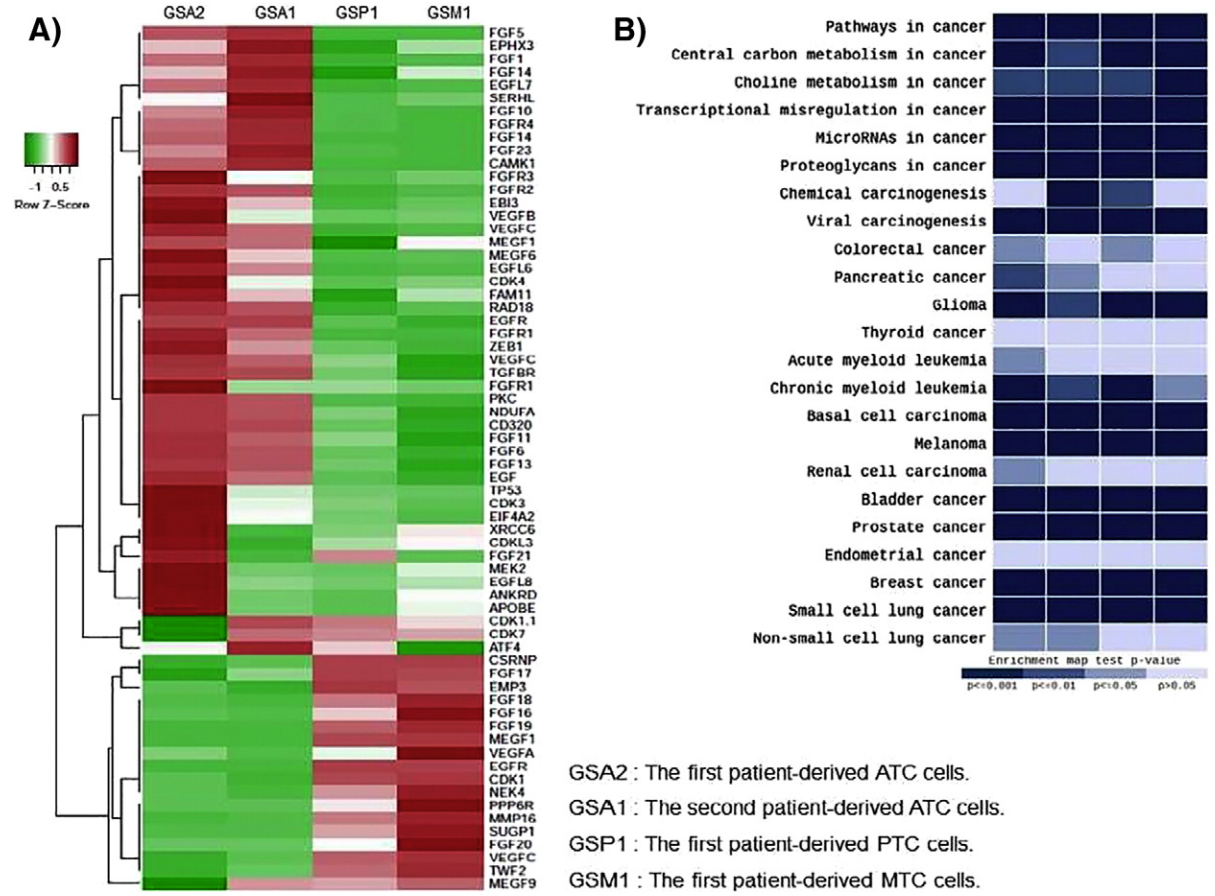

Figure 1. Gene expression profiles of patient-derived thyroid cancer cells. Gene expression analysis using a microarray approach in DTC and PDTC. (A) Gene expression profiles based on microarrays. (B) KEGG (Kyoto Encyclopedia of Genes and Genomes) pathway, expression patterns of genes related to human disease. Hierarchical clustering analysis for the comparison of DTC and PDTC.

HNHA and Lenvatinib in Combination Induced Apoptosis and Cell Cycle Arrest in Patient-Derived Thyroid Cancer Cells

Combined treatment with HNHA and lenvatinib showed the most significant induction of the sub-G_0G_1 population, resulting in the induction of cell death in GSP1, GSA1, and GSA2 cells (Figure 2*G–I*). The synergistic effect of HNHA and lenvatinib most potently induced the sub-G_0G_1 population, leading to apoptosis, cell cycle arrest, and strong inhibition of GSP1, GSA1, and GSA2 cell viability. Immunoblot analyses of protein levels in GSP1, GSA1, and GSA2 cell lines indicated that the HNHA and lenvatinib combination induced the most marked increases in the levels of p53 and p21, which are well-known arrestors of the cell cycle, and decreases in the levels of cyclin D1 and CDK 4, which are positive regulators of the cell cycle, as compared with responses to either agent alone or the combination of HNHA and sorafenib (Figure 2*J–L*). Of note, the proliferation marker (Ki-67) and anti-apoptotic (phosphorylated NF-κB, p65, and Bcl-2) markers were most highly suppressed in the HNHA and lenvatinib combination treatment group compared with groups treated with either agent alone or the combination of HNHA and sorafenib (Figure 2*J–L*). The expression of apoptotic markers (Apaf-1 and cleaved-caspase 3) were most highly induced in the HNHA and lenvatinib combination treatment group compared with groups treated with either agent alone or the combination of HNHA and sorafenib (Figure 2*J–L*). Together, these data indicate that the HNHA and lenvatinib combination effectively suppresses PDTC as well as DTC.

Drug Resistance of Cancer Stem Cells was Related to EMT Induction Mediated by FGFR Signaling Pathway Activation in GSP1, GSA1, and GSA2

We investigated whether the treatments inhibited EMT activation by the prevention of FGFR signal transduction. The FGFR signaling

Table 1. Cell Line Characteristics, Viability after Drug Treatment of All Thyroid Cancer Cell Lines Examined

	GSP1	GSA1	GSA2
Age at Diagnosis	31	74	56
Gender	Female	Female	Male
Primary Disease Site	Thyroid	Thyroid	Thyroid
Stage	IVc	IVc	IVc
Primary Pathology	Papillary thyroid cancer	Anaplastic thyroid cancer	Anaplastic thyroid cancer, resistance to Sorafenib
Classification of specimen used for culture	Fresh tumor	Fresh tumor	Fresh tumor
Obtained from	Gangnam Severance Hospital, Seoul, Korea	Gangnam Severance Hospital, Seoul, Korea	Gangnam Severance Hospital, Seoul, Korea

pathway is an evolutionarily conserved signaling cascade involved in various biological processes, including drug resistance. The combination of HNHA and lenvatinib had the greatest suppressive effects on the FGFR signaling pathway (PKC, MEK, and p-ERK1/2), and led to the inhibition of EMT (vimentin, snail, and zeb1) and dramatic increases in E-cadherin compared to either agent alone or the combination of HNHA and sorafenib in GSP1, GSA1, and GSA2 (Figure 2*M*–*O*). With respect to ligand binding, FGFR induced a cascade of downstream signaling pathways including mitogen-activated protein kinase enzymes MEK and ERK (in the MAPK pathway) and PKC, via PLCγ activation (Figure 2*M*–*O*).

These results suggest that more advanced cancer cells, CSCs, were more resistant to drugs through EMT induction mediated by FGFR signaling pathway activation. Synergistic effects of the HNHA and lenvatinib combination effectively suppressed EMT induction via the inhibition of the FGFR signaling pathway in GSP1, GSA1, and GSA2.

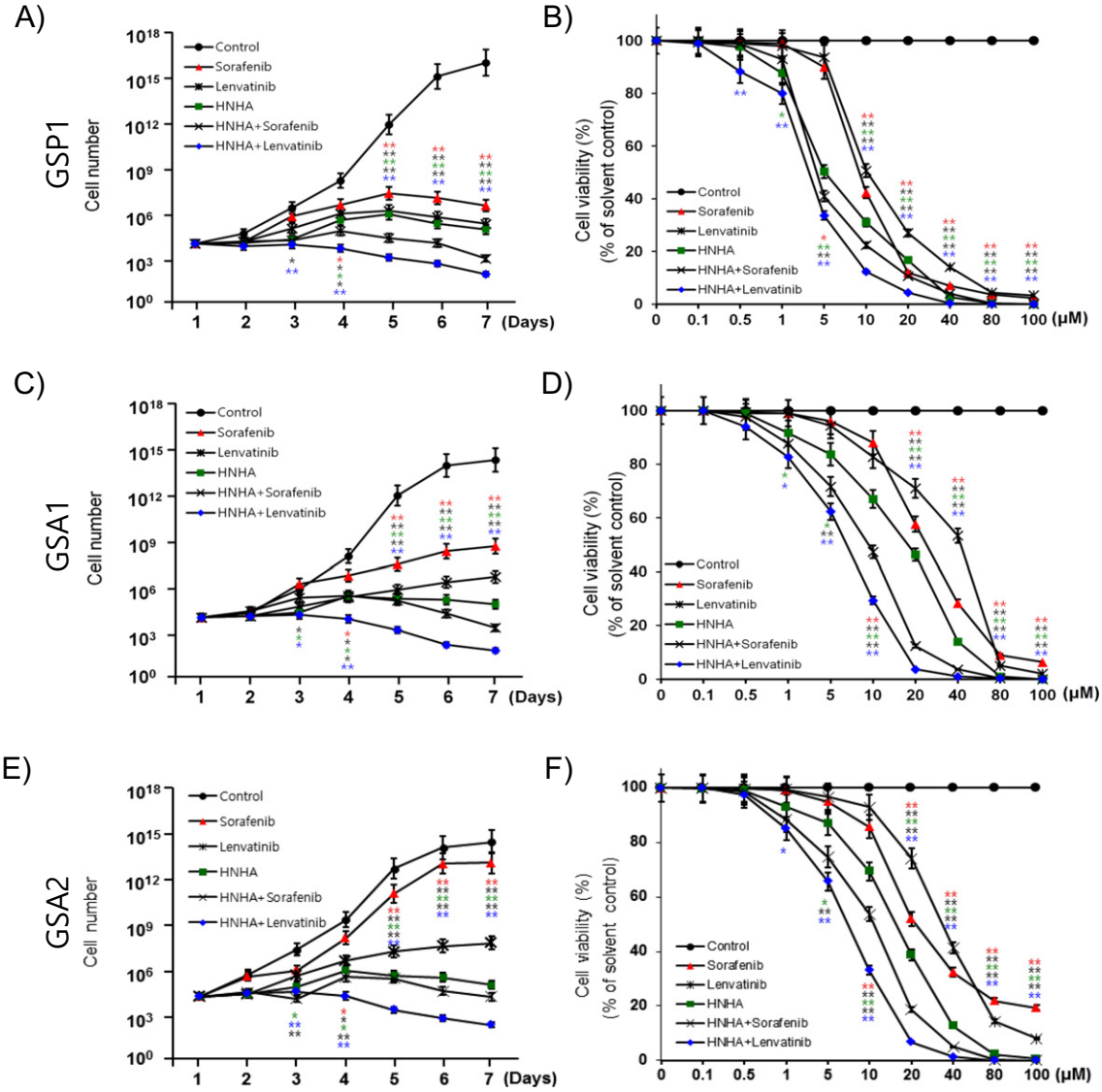

Figure 2. Synergistic anti-cancer effect of HNHA and lenvatinib on patient-derived thyroid cancer cells compared with the effects of each agent alone or HNHA and sorafenib in combination. Cell viability and proliferation assay of HNHA and lenvatinib combined, each agent alone, or HNHA and sorafenib combined in patient-derived thyroid cancer cells (GSP1, (A and B); GSA1, (C and D); GSA2, (E and F)). Points indicate mean % of the value observed in the solvent-treated control. All experiments were repeated at least 3 times. Data represent means ± SD. **P* < .05 vs. control, ***P* < .01 vs. control, ****P* < .005 vs. control. Cell cycle arrest induced by the combination of HNHA and lenvatinib (G, H and I). Cells were exposed to the indicated inhibitors, harvested, and stained with propidium iodide before analysis by flow cytometry and FlowJo v8. Immunoblot analysis about markers of cell cycle arrest, apoptosis, E-cadherin (negatively related to EMT), proliferation, cell cycle, anti-apoptosis activity, FGFR signaling pathway and EMT in patient-derived thyroid cancer cells (GSP1, (J and M); GSA1, (K and N); GSA2, (L and O)). GSP1, GSA1 and GSA2 were exposed to the indicated inhibitors for 24 hours prior to the analysis of the expression of Ki-67 (cell proliferation), Cyclin D1 and CDK4 (cell cycle), p21 and p53 (cell cycle arrest), Apaf-1 and cleaved-caspase 3 (apoptosis), p-NFκB and Bcl-2 (anti-apoptosis), PKC, MEK and phosphorylated ERK1/2 (FGFR signaling pathway), Vimentin, Snail, and Zeb1 (EMT), E-cadherin (loss of E-cadherin function promotes EMT) by immunoblotting.

G)

GSP1

Status	Sub-G_0G_1	G_0G_1	S	G_2/M
Control	2.4 ± 0.01	35.9 ± 0.03	34.8 ± 0.02	26.9 ± 0.02
Sorafenib only	18.4 ± 0.03	43.4 ± 0.04	22.6 ± 0.05	15.6 ± 0.02
Lenvatinib only	25.2 ± 0.02	45.5 ± 0.01	19.4 ± 0.02	9.9 ± 0.05
HNHA	33.4 ± 0.04	48.7 ± 0.01	11.4 ± 0.05	6.5 ± 0.05
HNHA+Sorafenib	61.4 ± 0.01	27.8 ± 0.06	6.8 ± 0.03	4.0 ± 0.03
HNHA+Lenvatinib	69.4 ± 0.02	23.7 ± 0.01	4.6 ± 0.01	2.3 ± 0.04

H)

GSA1

Status	Sub-G_0G_1	G_0G_1	S	G_2/M
Control	1.3 ± 0.02	45.5 ± 0.01	30.2 ± 0.03	23.0 ± 0.03
Sorafenib only	14.2 ± 0.01	46.3 ± 0.02	20.0 ± 0.02	19.5 ± 0.03
Lenvatinib only	19.5 ± 0.04	49.5 ± 0.02	15.8 ± 0.05	15.2 ± 0.06
HNHA	26.8 ± 0.05	46.7 ± 0.02	15.9 ± 0.05	10.6 ± 0.01
HNHA+Sorafenib	51.8 ± 0.05	31.5 ± 0.04	11.5 ± 0.02	5.2 ± 0.06
HNHA+Lenvatinib	67.2 ± 0.05	21.3 ± 0.05	8.2 ± 0.04	3.3 ± 0.02

I)

GSA2

Status	Sub-G_0G_1	G_0G_1	S	G_2/M
Control	0.7 ± 0.05	41.2 ± 0.02	41.9 ± 0.02	16.2 ± 0.04
Sorafenib only	4.5 ± 0.02	40.8 ± 0.01	39.7 ± 0.03	15.0 ± 0.01
Lenvatinib only	15.9 ± 0.02	48.4 ± 0.05	26.2 ± 0.03	9.5 ± 0.01
HNHA	23.4 ± 0.01	51.3 ± 0.03	20.5 ± 0.01	4.8 ± 0.04
HNHA+Sorafenib	45.7 ± 0.02	35.4 ± 0.01	14.8 ± 0.05	4.1 ± 0.02
HNHA+Lenvatinib	59.3 ± 0.02	30.7 ± 0.03	7.9 ± 0.02	2.1 ± 0.01

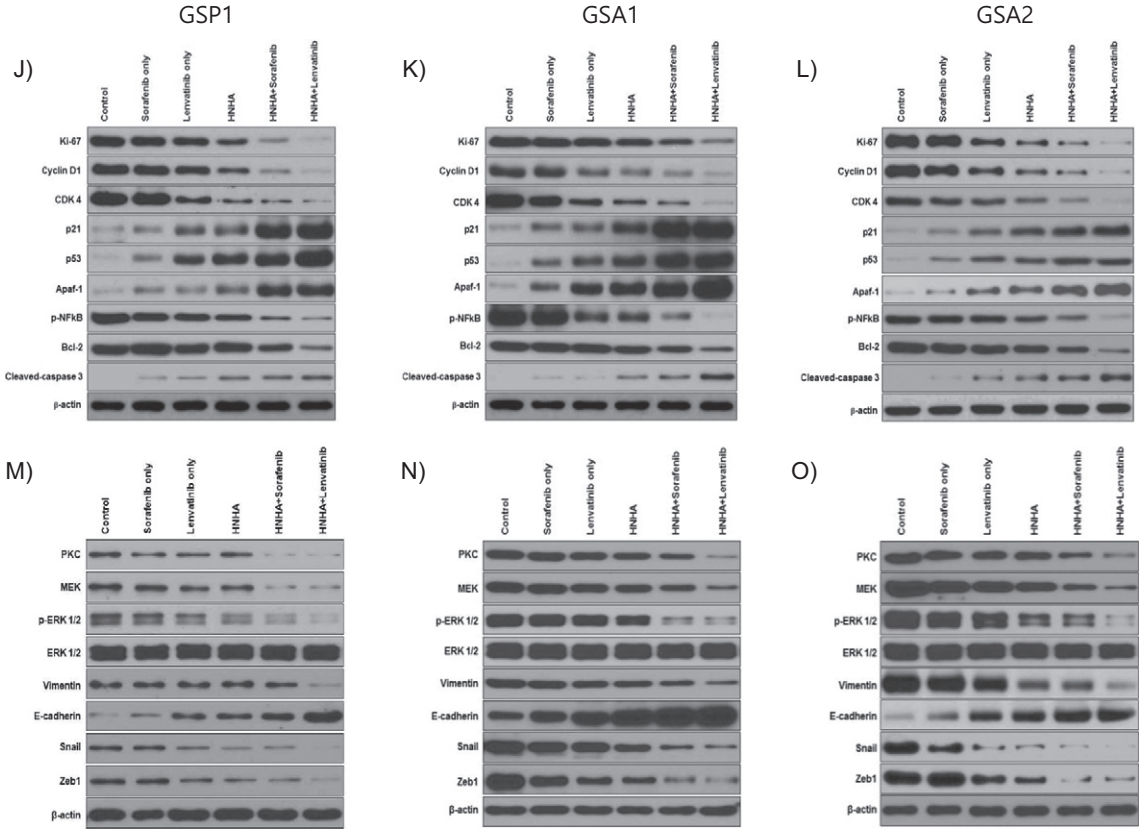

Figure 2. *(continued).*

Table 2. IC50 (half maximal inhibitory concentration) Determination Using a Cell Proliferation Assay. HNHA and Lenvatinib Combination Treatment is a Lower IC50 than HNHA and Sorafenib Combination or Sorafenib, Lenvatinib and HNHA Alone. Each Data point Represents the Mean of 3 Independent MTT Assays for IC50 Performed in Triplicate. SD, standard deviation

Cell Line	Hisopathology	Animal	Cell Proliferation IC_{50}^{*}) (μM)				
			Sorafenib	Lenvatinib	HNHA	HNHA ± S	HNHA ± L
GSP1	Thyroid cancer: Papillary	Human	9.42 (± 0.2)	10.51 (± 0.1)	5.15 (± 0.4)	4.95 (± 0.5)	3.84 (± 0.3) *
GSA1	Thyroid cancer: Anaplastic	Human	23.51 (± 0.2)	41.54 (± 0.5)	20.05 (± 0.4)	9.63 (± 0.1)	6.49 (± 0.2) *
GSA2	Thyroid cancer: Anaplastic	Human	21.11 (± 0.3)	35.13 (± 0.2)	18.33 (± 0.3)	11.47 (± 0.5)	7.32 (± 0.5) *

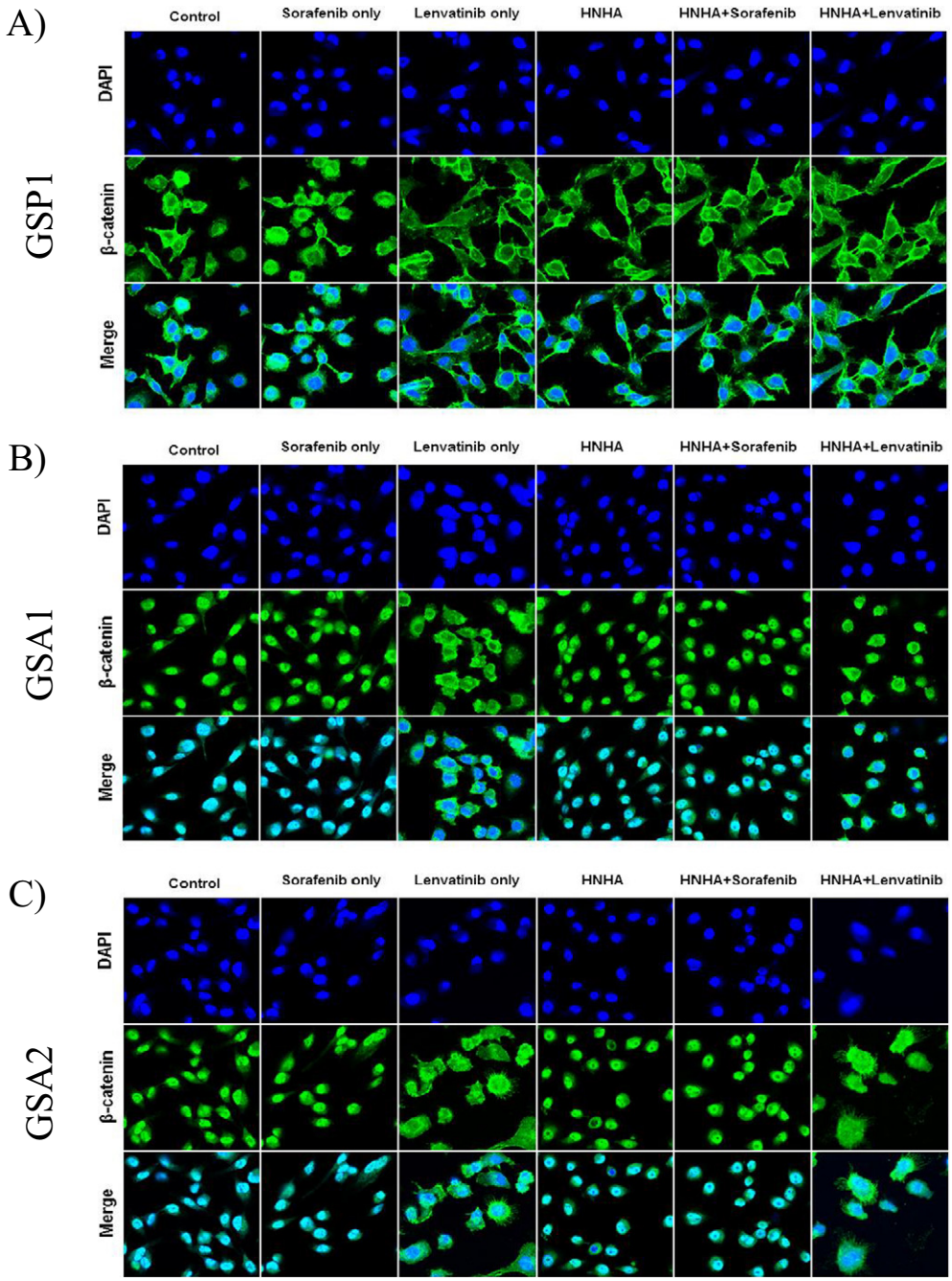

Figure 3. Lenvatinib prevents EMT through repression of β-catenin nuclear translocation in GSA1 and GSA2 cancer stem-like cells. Immunofluorescence cytochemical staining showed that β-catenin nuclear localization was greater in GSA1 (B) and GSA2 (C) cancer stem-like cells, than in GSP1 (A). However, these cells were sensitive to EMT inhibition via β-catenin nuclear localization by lenvatinib.

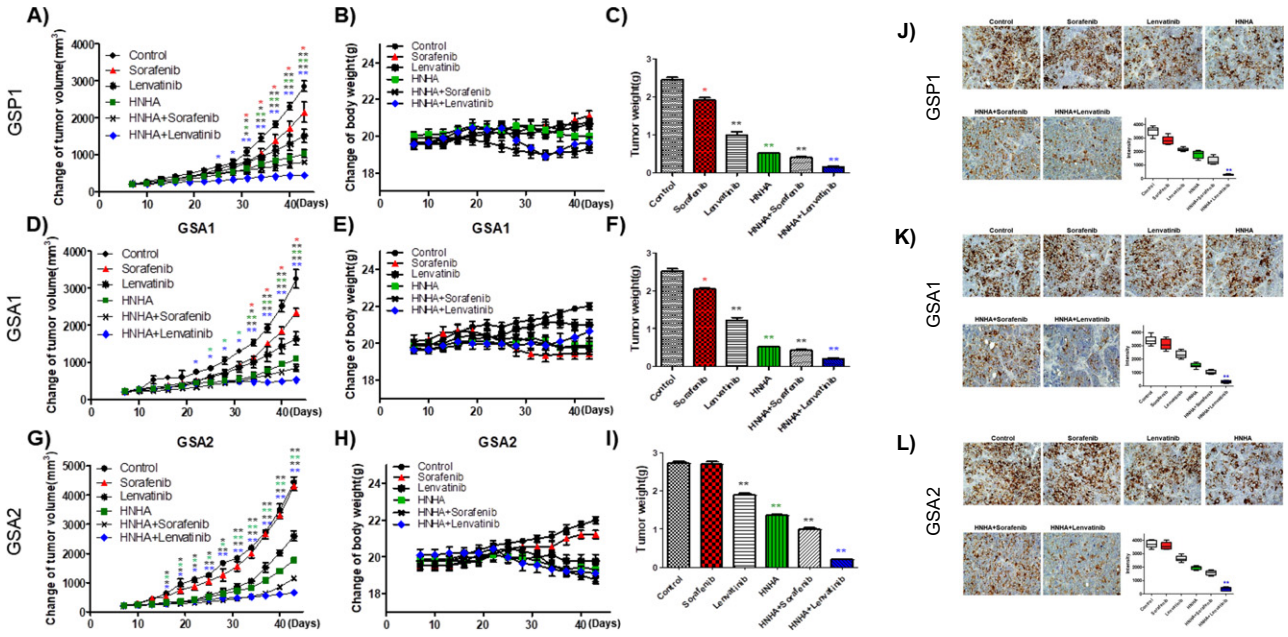

Figure 4. Combination of HNHA and lenvatinib produced synergistic anti-cancer effects in patient-derived thyroid cancer cell xenografts in vivo. Athymic nude mice with established tumors were treated with the indicated inhibitors. Data represent the mean tumor volumes. Inhibition of tumor progression by combination therapy of the HNHA and lenvatinib in mice with patient-derived thyroid cancer cell (GSP1, A–C; GSA1, D–F; and GSA2, G–I) xenografts (n = 10 mice/group). Change of tumor volume (A, D, and G). The compounds had no significant effect on mouse body weight (B, E, and H). Weight of dissected tumors (C, F, and I). Immunohistochemical analysis of Bcl-2 protein levels in paraffin-embedded tumor tissues from mice with GSP1, GSA1, and GSA2 xenografts (J, K, and L). Synergistic activity of the HNHA and lenvatinib combination induced more potent inhibition of tumor Bcl-2 expression than each agent used alone or HNHA and sorafenib in combination. MetaMorph 4.6 image-analysis software was used to quantify Bcl-2 immunostaining. *P < .05; **P < .01; ***P < .005 for the comparison with the control.

β-Catenin, an EMT Marker, Plays a Key Role in EMT Induction by Nuclear Localization on Advanced Thyroid Cancer Cells

β-Catenin constitutes a well-known, conserved regulatory factor with a crucial role in a tumorigenesis that is correlated with a poor prognosis. β-Catenin nuclear localization acts synergistically to promote the expression of target genes related to drug resistance. PDTC CSCs acquired drug resistance via EMT activation mediated by β-catenin nuclear localization. In GSA1 and 2, patient-derived anaplastic thyroid cancer 1 and 2, β-catenin nuclear localization was greater than that in patient-derived papillary thyroid cancer 1, GSP1 (Figure 3*A*–*C*, each control panel). β-Catenin nuclear localization in GSA1 and 2 was significantly inhibited by the FGFR inhibitor lenvatinib as opposed to non-FGFR inhibitors, HNHA or sorafenib (Figure 3*A*–*C*). These results indicate that the disruption of EMT activation via FGFR signaling pathway inhibition contributed to the efficacy against drug resistance by lenvatinib.

Significant Tumor Shrinkage was Induced by the Combination of HNHA and Lenvatinib in a Xenograft Model

To investigate the synergistic anti-cancer effect of the combination of HNHA and lenvatinib in vivo, we developed a mouse xenograft tumor model using patient-derived papillary thyroid cancer cells, GSP1, GSA1, and GSA2. Each agent used alone and the combination of HNHA and sorafenib did not markedly suppress GSP1, GSA1, and GSA2 cell xenograft tumors; however, the combination of HNHA and lenvatinib resulted in tumor suppression (Figure 4*A*, *D*, and *G*). Moreover, there was no evidence for systemic toxicity or treatment-related death in any group. Mouse body weight was not significantly influenced by treatment with sorafenib, lenvatinib, or HNHA (Figure 4*B*, *E*, and *H*). The HNHA and lenvatinib combination treatment group had significantly smaller tumor volumes than those of mice treated with each agent used alone or the combination of HNHA and sorafenib (Figure 4*C*, *F*, and *I*). As anti-apoptotic activity is a fundamental factor in the evaluation of tumorigenesis and Bcl-2 serves as an important marker of anti-apoptotic activity, we identified this marker by immunohistochemistry analysis of GSP1, GSA1, and GSA2 cell xenograft tumors. This demonstrated that the HNHA and lenvatinib combination treatment group showed the strongest decrease in Bcl-2 expression among all groups (Figure 4*J*–*L*). Accordingly, the HNHA and lenvatinib combination treatment was considered to have potent anti-cancer effects in CSCs of PDTC as well as in the DTC xenograft model.

Discussion

EMT is linked to cancer growth, including metastasis, therapeutic resistance, and recurrence. CSCs, which are found in poorly differentiated tumors and have stem cell-like features [21], have the capacity for self-renewal and are associated with metastases and therapeutic resistance [22]. Recent studies have demonstrated a link between EMT, drug resistance, and CSCs [23]. In particular, CSCs and EMT-type cells, which share some molecular characteristics with CSCs, are believed to perform crucial roles in drug resistance and cancer metastasis, as observed in some malignant cancers in humans [23]. EMT is associated with the gain of stem cell-like properties and

is sufficient to provide differentiated normal and cancer cells with stem cell properties. Furthermore, CSCs frequently also exhibit EMT properties. Numerous studies have examined the relationship between EMT and drug resistance in CSCs. In the present study, we investigated EMT-mediated drug resistance via the FGFR signaling pathway in patient-derived anaplastic thyroid cancer cells, a type of cancer stem-like cells. These cells exhibited high expression of markers of the EMT and FGFR signaling pathway. Some studies have shown that FGF2 and β3 integrin are part of an EMT signature that contributes to FGFR1-mediated drug resistance and metastatic progression [15]. Drug resistance of CSCs was dependent on the EMT-associated FGFR signaling pathway. Consequently, we focused on the effect of inhibition of the FGFR signaling pathway by tyrosine kinase inhibitors (TKIs) on CSCs.

TKIs are suggested in patients with radioiodine-refractory DTC with metastatic, rapidly progressive, symptomatic, and/or imminently threatening disease that is not otherwise amenable to local control with other approaches. Systemic therapeutics resulted in improved progression-free survival in three randomized, double-blinded, placebo-controlled clinical trials, i.e., vandetanib, sorafenib, and lenvatinib [24–26]. Sorafenib inhibits RAF-1, a member of the RAF/MEK/ERK signaling pathway, BRAF activity, and VEGFR-2, VEGFR-3, PDGFR-β, and c-KIT [27]. Lenvatinib has a potent inhibitory effect on VEGFR-2, VEGFR-3, PDGFRα/β, KIT, and RET, as well as, unlike sorafenib, FGFR 1–4. The most important difference between lenvatinib and other drugs is the ability to inhibit FGFR 1, establishing it as an effective drug in cases in which resistance to VEGFR inhibitors develops [28–30]. Although both lenvatinib and sorafenib show good results in phase III trials and are the first-line treatment in radioiodine-refractory DTCs, most patients eventually stop responding to these agents, and many are not able to continue medication owing to their toxicity. In patients who exhibit disease progression during initial kinase inhibitor therapy, without prohibitive adverse effects, only lenvatinib may be used as a second-line treatment [24]. Several mechanisms explain TKI resistance, such as receptor autophosphorylation, autophagy, hypoxia-inducing factor, epigenetic regulation, and EMT [31,32]. There are several EMT-inducing cytokines, e.g., TGF-β, FGF, HGF, insulin-like growth factor, and IL-6 [33,34]. EMT in thyroid cancer is induced in more aggressive forms, with increased expression of ZEB1, which can promote drug resistance via EMT-dependent and EMT-independent mechanisms [35–37]. Studies have shown that the down-regulation of ZEB1 expression could restore drug sensitivity [38,39]. For example, sorafenib inhibits EMT in hepatocellular carcinoma, attenuates HGF secretion in polarized macrophages, and decreases plasma HGF. Sorafenib also abolishes polarized-macrophage-induced activation of the HGF receptor Met [40]. Notably, reversion of EMT overcomes drug resistance in lung adenocarcinoma [33].

The present study demonstrated that the drug resistance of CSC-like cancer cells, i.e., sorafenib-resistant-patient derived thyroid cancer cells, was inhibited by combination therapy with HNHA and lenvatinib through the inhibition of the EMT-mediated FGFR signaling pathway. Synergistic effects of HNHA and lenvatinib were more efficient than the effects of either agent used singly or the combination of HNHA and sorafenib. The combined treatment effectively induced markers of cell cycle arrest and apoptosis and reduced anti-apoptosis markers, EMT, and the FGFR signaling pathway. In addition to cell culture studies, in vivo studies using a xenograft model indicated significant tumor shrinkage in the HNHA and lenvatinib combined treatment group. We propose that these effects might be explained by reduced EMT-mediated drug resistance in CSCs. Specifically, the combination of HNHA and lenvatinib blocked the FGFR signaling pathway, which is important for EMT and metastasis [41]. Notably, these findings indicate that the combination of HNHA and lenvatinib is a potentially effective new clinical approach for the care of patients with CSCs with drug-resistant properties.

Acknowledgments

The authors thank Dr. Seung Won Kim for critical brainstorming and Dr. Kyung Hwa Choi for assistance with tumor cell isolation from the patient specimens.

References

[1] Nikiforov YE (2008). Thyroid carcinoma: molecular pathways and therapeutic targets. *Mod Pathol* **21**(Suppl 2), S37–43.

[2] Ferrari SM, Fallahi P, Politti U, Materazzi G, Baldini E, Ulisse S, Miccoli P, and Antonelli A (2015). Molecular Targeted Therapies of Aggressive Thyroid Cancer. *Front Endocrinol (Lausanne)* **6**, 176.

[3] Saiselet M, Floor S, Tarabichi M, Dom G, Hebrant A, van Staveren WC, and Maenhaut C (2012). Thyroid cancer cell lines: an overview. *Front Endocrinol (Lausanne)* **3**, 133.

[4] Xing M (2013). Molecular pathogenesis and mechanisms of thyroid cancer. *Nat Rev Cancer* **13**, 184–199.

[5] Xing M (2009). Identifying genetic alterations in poorly differentiated thyroid cancer: a rewarding pursuit. *J Clin Endocrinol Metab* **94**, 4661–4664.

[6] Cherkaoui GS, Guensi A, Taleb S, Idir MA, Touil N, Benmoussa R, Baroudi Z, and Chikhaoui N (2015). Poorly differentiated thyroid carcinoma: a retrospective clinicopathological study. *Pan Afr Med J* **21**, 137.

[7] Abe I, Karasaki S, Matsuda Y, Sakamoto S, Nakashima T, Yamamoto H, Kawate H, Ohnaka K, Nakashima H, and Kobayashi K, et al (2015). Complete remission of anaplastic thyroid carcinoma after concomitant treatment with docetaxel and radiotherapy. *Case Rep Endocrinol* **2015**, 726085.

[8] Grygielewicz P, Dymek B, Bujak A, Gunerka P, Stanczak A, Lamparska-Przybysz M, Wieczorek M, Dzwonek K, and Zdzalik D (2016). Epithelial-mesenchymal transition confers resistance to selective FGFR inhibitors in SNU-16 gastric cancer cells. *Gastric Cancer* **19**, 53–62.

[9] Housman G, Byler S, Heerboth S, Lapinska K, Longacre M, Snyder N, and Sarkar S (2014). Drug resistance in cancer: an overview. *Cancers (Basel)* **6**, 1769–1792.

[10] Wendt MK, Tian M, and Schiemann WP (2012). Deconstructing the mechanisms and consequences of TGF-beta-induced EMT during cancer progression. *Cell Tissue Res* **347**, 85–101.

[11] Stuhlmiller TJ, Miller SM, Zawistowski JS, Nakamura K, Beltran AS, Duncan JS, Angus SP, Collins KA, Granger DA, and Reuther RA, et al (2015). Inhibition of Lapatinib-Induced Kinome Reprogramming in ERBB2-Positive Breast Cancer by Targeting BET Family Bromodomains. *Cell Rep* **11**, 390–404.

[12] Singh A and Settleman J (2010). EMT, cancer stem cells and drug resistance: an emerging axis of evil in the war on cancer. *Oncogene* **29**, 4741–4751.

[13] Wendt MK, Taylor MA, Schiemann BJ, Sossey-Alaoui K, and Schiemann WP (2014). Fibroblast growth factor receptor splice variants are stable markers of oncogenic transforming growth factor beta1 signaling in metastatic breast cancers. *Breast Cancer Res* **16**, R24.

[14] Warzecha CC, Jiang P, Amirikian K, Dittmar KA, Lu H, Shen S, Guo W, Xing Y, and Carstens RP (2010). An ESRP-regulated splicing programme is abrogated during the epithelial-mesenchymal transition. *EMBO J* **29**, 3286–3300.

[15] Brown WS, Tan L, Smith A, Gray NS, and Wendt MK (2016). Covalent Targeting of Fibroblast Growth Factor Receptor Inhibits Metastatic Breast Cancer. *Mol Cancer Ther* **15**, 2096–2106.

[16] Brown WS, Akhand SS, and Wendt MK (2016). FGFR signaling maintains a drug persistent cell population following epithelial-mesenchymal transition. *Oncotarget* **7**, 83424–83436.

[17] Shibue T and Weinberg RA (2017). EMT, CSCs, and drug resistance: the mechanistic link and clinical implications. *Nat Rev Clin Oncol* **10**, 611–629

[18] Bernet V and Smallridge R (2014). New therapeutic options for advanced forms of thyroid cancer. *Expert Opin Emerg Drugs* **19**, 225–241.
[19] Ma R, Minsky N, Morshed SA, and Davies TF (2014). Stemness in human thyroid cancers and derived cell lines: the role of asymmetrically dividing cancer stem cells resistant to chemotherapy. *J Clin Endocrinol Metab* **99**, E400-09.
[20] Mani SA, Guo W, Liao MJ, Eaton EN, Ayyanan A, Zhou AY, Brooks M, Reinhard F, Zhang CC, and Shipitsin M, et al (2008). The epithelial-mesenchymal transition generates cells with properties of stem cells. *Cell* **133**, 704–715.
[21] Liu X and Fan D (2015). The epithelial-mesenchymal transition and cancer stem cells: functional and mechanistic links. *Curr Pharm Des* **21**, 1279–1291.
[22] Borah A, Raveendran S, Rochani A, Maekawa T, and Kumar DS (2015). Targeting self-renewal pathways in cancer stem cells: clinical implications for cancer therapy. *Oncogene* **4**, e177.
[23] Sarkar FH, Li Y, Wang Z, and Kong D (2009). Pancreatic cancer stem cells and EMT in drug resistance and metastasis. *Minerva Chir* **64**, 489–500.
[24] Haugen BR, Alexander EK, Bible KC, Doherty GM, Mandel SJ, Nikiforov YE, Pacini F, Randolph GW, Sawka AM, and Schlumberger M, et al (2016). 2015 American Thyroid Association Management Guidelines for Adult Patients with Thyroid Nodules and Differentiated Thyroid Cancer: The American Thyroid Association Guidelines Task Force on Thyroid Nodules and Differentiated Thyroid Cancer. *Thyroid* **26**, 1–133.
[25] Schlumberger M, Tahara M, Wirth LJ, Robinson B, Brose MS, Elisei R, Habra MA, Newbold K, Shah MH, and Hoff AO, et al (2015). Lenvatinib versus placebo in radioiodine-refractory thyroid cancer. *N Engl J Med* **372**, 621–630.
[26] Brose MS, Nutting CM, Jarzab B, Elisei R, Siena S, Bastholt L, de la Fouchardiere C, Pacini F, Paschke R, and Shong YK, et al (2014). Sorafenib in radioactive iodine-refractory, locally advanced or metastatic differentiated thyroid cancer: a randomised, double-blind, phase 3 trial. *Lancet* **384**, 319–328.
[27] Wilhelm SM, Carter C, Tang L, Wilkie D, McNabola A, Rong H, Chen C, Zhang X, Vincent P, and McHugh M, et al (2004). BAY 43-9006 exhibits broad spectrum oral antitumor activity and targets the RAF/MEK/ERK pathway and receptor tyrosine kinases involved in tumor progression and angiogenesis. *Cancer Res* **64**, 7099–7109.
[28] Glen H, Mason S, Patel H, Macleod K, and Brunton VG (2011). E7080, a multi-targeted tyrosine kinase inhibitor suppresses tumor cell migration and invasion. *BMC Cancer* **11**, 309.
[29] Tohyama O, Matsui J, Kodama K, Hata-Sugi N, Kimura T, Okamoto K, Minoshima Y, Iwata M, and Funahashi Y (2014). Antitumor activity of lenvatinib (e7080): an angiogenesis inhibitor that targets multiple receptor tyrosine kinases in preclinical human thyroid cancer models. *J Thyroid Res* **2014**, 638747.
[30] Lorusso L, Pieruzzi L, Biagini A, Sabini E, Valerio L, Giani C, Passannanti P, Pontillo-Contillo B, Battaglia V, and Mazzeo S, et al (2016). Lenvatinib and other tyrosine kinase inhibitors for the treatment of radioiodine refractory, advanced, and progressive thyroid cancer. *Onco Targets Ther* **9**, 6467–6477.
[31] Zhu YJ, Zheng B, Wang HY, and Chen L (2017). New knowledge of the mechanisms of sorafenib resistance in liver cancer. *Acta Pharmacol Sin* **38**, 614–622.
[32] Adjibade P, St-Sauveur VG, Quevillon Huberdeau M, Fournier MJ, Savard A, Coudert L, Khandjian EW, and Mazroui R (2015). Sorafenib, a multikinase inhibitor, induces formation of stress granules in hepatocarcinoma cells. *Oncotarget* **6**, 43927–43943.
[33] Kurimoto R, Iwasawa S, Ebata T, Ishiwata T, Sekine I, Tada Y, Tatsumi K, Koide S, Iwama A, and Takiguchi Y (2016). Drug resistance originating from a TGF-beta/FGF-2-driven epithelial-to-mesenchymal transition and its reversion in human lung adenocarcinoma cell lines harboring an EGFR mutation. *Int J Oncol* **48**, 1825–1836.
[34] Qi L, Song W, Li L, Cao L, Yu Y, Song C, Wang Y, Zhang F, Li Y, and Zhang B, et al (2016). FGF4 induces epithelial-mesenchymal transition by inducing store-operated calcium entry in lung adenocarcinoma. *Oncotarget* **7**, 74015–74030.
[35] Montemayor-Garcia C, Hardin H, Guo Z, Larrain C, Buehler D, Asioli S, Chen H, and Lloyd RV (2013). The role of epithelial mesenchymal transition markers in thyroid carcinoma progression. *Endocr Pathol* **24**, 206–212.
[36] Lan L, Luo Y, Cui D, Shi BY, Deng W, Huo LL, Chen HL, Zhang GY, and Deng LL (2013). Epithelial-mesenchymal transition triggers cancer stem cell generation in human thyroid cancer cells. *Int J Oncol* **43**, 113–120.
[37] Zhang P, Sun Y, and Ma L (2015). ZEB1: at the crossroads of epithelial-mesenchymal transition, metastasis and therapy resistance. *Cell Cycle* **14**, 481–487.
[38] Meidhof S, Brabletz S, Lehmann W, Preca BT, Mock K, Ruh M, Schuler J, Berthold M, Weber A, and Burk U, et al (2015). ZEB1-associated drug resistance in cancer cells is reversed by the class I HDAC inhibitor mocetinostat. *EMBO Mol Med* **7**, 831–847.
[39] Zhou G, Zhang F, Guo Y, Huang J, Xie Y, Yue S, Chen M, Jiang H, and Li M (2017). miR-200c enhances sensitivity of drug-resistant non-small cell lung cancer to gefitinib by suppression of PI3K/Akt signaling pathway and inhibites cell migration via targeting ZEB1. *Biomed Pharmacother* **85**, 113–119.
[40] Deng YR, Liu WB, Lian ZX, Li X, and Hou X (2016). Sorafenib inhibits macrophage-mediated epithelial-mesenchymal transition in hepatocellular carcinoma. *Oncotarget* **7**, 38292–38305.
[41] Ryu SH, Heo SH, Park EY, Choi KC, Ryu JW, Lee SH, and Lee SW (2017). Selumetinib Inhibits Melanoma Metastasis to Mouse Liver via Suppression of EMT-targeted Genes. *Anticancer Res* **37**, 607–614.